Community-Aware Dynamic Graph Learning for Brain Disorder Diagnosis

Qiuyan Li[1,†], Guangming Li[1,†], Wei Yu[2], Guanxun Cheng[3], Keyan Yu[3], Xiang Fan[3,*], and Kai Wang[1,*]

[1] School of Computer Science and Technology, Dongguan University of Technology, Dongguan, 523808, China
[2] School of Computer Science, Wuhan University, Wuhan 430072, China
[3] Department of Medical Imaging, Peking University Shenzhen Hospital, Shenzhen, 518172, China
† Co-first Authors
* Corresponding Author: (fiona@link.cuhk.edu.hk and kevin.w@dgut.edu.cn)

Abstract. Functional MRI (fMRI)-derived dynamic brain functional connectivity (dBFC) holds significant potential for characterizing brain disorder-specific abnormalities in macroscopic neural activity patterns underlying cognition and behavior. Yet, standard approaches usually estimate connectivity via zero-lag correlations. This simplification ignores temporal lags among different brain regions, which are biologically meaningful markers of directed neural propagation and diverse pathological brain states. Furthermore, existing graph learning models often underexploit the brain's hierarchical modular architecture and struggle to capture disorder-induced community switching of brain regions between functional modules. In this work, we propose the Community-aware Dynamic Graph Neural Network (CaDGNN) framework to learn the spatiotemporal interaction patterns in lag-aware dBFC networks for brain disorder diagnosis. First, CaDGNN incorporates a lag-aware dBFC network construction module to encode spatiotemporal propagation patterns of brain activation by explicitly incorporating inter-regional time delays. Then, a temporal community co-occurrence encoder is introduced to extract temporal community structures and model dynamic inter-regional interactions. Based on this, a dual-level dynamic learning module models the switching behavior of graph nodes between communities and the temporal evolution of community structures simultaneously for final diagnosis. Evaluations on four independent datasets demonstrate that CaDGNN outperforms state-of-the-art methods. Our findings highlight the diagnostic value of incorporating both lag-aware dynamics and modular structure into graph learning. The codes of CaDGNN are available at https://github.com/Alyrrraa/CaDGNN.

Keywords: Brain disorder diagnosis · Graph Transformer · Dynamic brain functional connectivity · Delayed connectivity.

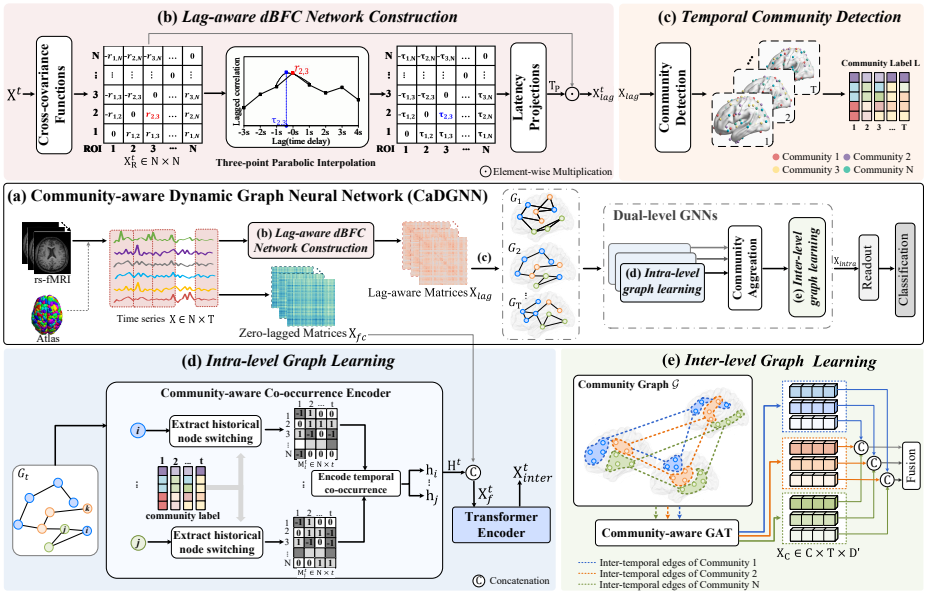

Fig. 1: The overall architecture of the proposed CaDGNN (a), including the lag-aware dBFC network construction module (b), the temporal community detection module (c), and the dual-level GNNs with intra-level (d) and inter-level graph learning (e).

1 Introduction

The human brain operates as a complex, non-stationary system where spatially segregated brain regions continuously coordinate through dynamic reorganization to support cognition and behavior [1,3]. To investigate these complex dynamics, magnetic resonance imaging (MRI), especially resting-state functional MRI (rs-fMRI), has emerged as a powerful technique to estimate neural activity over time by measuring the low-frequency spontaneous fluctuations in blood-oxygen-level-dependent (BOLD) signals [17]. Unlike static connectivity, rs-fMRI-derived dynamic brain functional connectivity (dBFC) captures the temporal variability of neural interactions, offering a more fine-grained view of how spatiotemporal communication within BFC networks is organized, and more importantly, how its disruption contributes to diverse brain disorders [10].

Generally, existing dBFC-based methods estimate time-resolved interregional functional connectivity based on a sliding window mechanism, generating a sequence of graph structures where egions of interest (ROIs) corresponding to time windows and edges denote functional connectivity strength. Consequently, brain disorder diagnosis is often formulated as a graph classification problem. Following this line, state-of-the-art methods favor a decoupled learning strategy: Graph Neural Networks (GNNs) extract spatial patterns from individual temporal graphs, followed by sequence models (e.g., Transformers or Recurrent

Neural Networks (RNNs)) that aggregate temporal dynamics across time window sequences [4,16,14].

While effective, existing dBFC modeling paradigms suffer from critical limitations that restrict their diagnostic performance. *First*, most existing methods rely on the zero-lag functional connectivity assumption to construct dBFC graphs, where neural interactions are treated as instantaneous. However, neurophysiological evidence suggests that infra-slow electrophysiological activity propagates across the cortex in a widespread and stereotyped pattern, yielding reliable interregional time delays [20,18,23]. Explicitly modeling these delays in dBFC networks would better characterize abnormal neural propagation arising from disrupted and lagged brain activities. *Second*, the brain exhibits a hierarchical modular organization (i.e., community structure) that balances functional integration and segregation [22,32]. Exploring how individual ROIs fluctuate between communities over time could reveal disorder-specific biomarkers [32], which have been seldom investigated yet. *Last but not least*, integrating the intrinsic spatiotemporal coupling of dBFC networks into a unified framework remains challenging, given the brain's structural complexity and non-stationary dynamics.

To address these, we propose the Community-aware Dynamic Graph Neural Network (CaDGNN), a novel spatiotemporal graph neural network designed to diagnose brain disorders by modeling spatiotemporal interaction patterns within lag-aware dBFC networks. As illustrated in Fig. 1, we start by constructing lag-aware dBFC networks that explicitly encode inter-regional time delays. Then, we introduce a mechanism to extract temporal community structures, allowing the model to track the dynamic affiliation of brain regions to functional modules. Finally, a dual-level learning module characterizes both the node-level switching behavior within communities and inter-community temporal dynamics to perform robust classification.

The major contributions of this work are summarized as follows: (i) we introduce a lag-aware dBFC network construction strategy that incorporates intrinsic signal delays to characterize the spatiotemporal propagation of brain activity; (ii) we design a temporal community co-occurrence encoder to capture the dynamic interplay between ROIs by tracking their evolving community memberships; and (iii) we develop a dual-level dynamic learning module that jointly models intra-community node switching and inter-community evolution, significantly improving diagnostic performance across four independent datasets.

2 Method

2.1 Community-aware dBFC Graph Construction

Lag-aware dBFC Network Construction Inspired by previous studies [19,23], we perform time delay estimation to characterize the sequential propagation of brain activity. For each subject, BOLD signals are averaged within each ROI and divided into T segments using sliding windows. Within each segment

$t = 1, \ldots, T$, lagged correlations $r_{i,j}$ between ROIs i and j are computed using the cross-covariance function (CCF). To obtain a temporal resolution finer than the original sampling interval, three-point parabolic interpolation is then applied to the CCF curve to estimate the peak value $r_{i,j}$ and the corresponding time delay $\tau_{i,j}$. All delays are then projected onto one-dimensional maps, formulated as $T_p = (1/N)\left[\sum_{j=1}^{N} \tau_{1,j}, \ldots, \sum_{j=1}^{N} \tau_{N,j}\right]$, where N is the number of ROIs. We define the lag-aware FC matrix X_{lag}^t by weighting $X_R^t \in \mathbb{R}^{N \times N}$ with T_p to reflect spatiotemporal patterns. In parallel, the zero-lag FC matrix X_{fc}^t is computed by Pearson correlation, as strong zero-lag correlations constitute the backbone of functional brain networks [26].

Temporal Community Detection Incorporating the property of modular community structure during node propagation learning process would enable the model to better reflect brain's natural organization [9,22]. Accordingly, we propose a temporal community detection (TCD) strategy to identify communities in lag-aware dBFC networks. Specifically, we apply multilayer network analysis [21,24] to the lag-aware dBFC networks and obtain the optimal community structures $C \in \mathbb{R}^{N \times T}$ by optimizing the modularity quality function Q:

$$Q = \frac{1}{2\mu} \sum_{ijtr} \left[B_{ij}^t \delta(t,r) + \delta(i,j)\omega_j^t \right] \delta(M_i^t, M_j^r) \tag{1}$$

where the indicator function $\delta(M_i^t, M_j^r) = 1$ if nodes i and j belong to the same module, and $B = \left(X_{lag}^+ - \gamma P^+\right) - \left(X_{lag}^- - \gamma P^-\right)$ denotes the signed modularity matrix. Here, P is the expected weight of connections between nodes. γ and ω are the topological resolution and the temporal coupling parameters between adjacent time segments t and r. X^+ and X^- denote positive and negative connections. Based on C, we further obtain a community label set L, each element of which indicates community assignment of each node at segment t.

2.2 Dual-level Graph Neural Networks

Intra-level Graph Learning For each subject, we formulate T lag-aware dBFC networks as a graph set $G = \{G(1), G(2), \ldots, G(T)\}$. Each graph at segment t can be represented as $G(t) = (V(t), X_{lag}(t), A(t))$, where $V(t)$, $A(t)$, $X_{lag}(t)$ denote the set of nodes, the adjacency matrix, and the feature matrix, respectively. The dynamic graph sequence $\{G_t\}_{t=1}^T$ is input to the proposed intra-level graph learning module, with two components:

1) community-aware co-occurrence encoder Considering that nodes within the same community exhibit similar switching pattern and are tightly coupled during network reconfiguration [33], we introduce a community-aware encoder (CCE) to model historical activity sequences. For each node i in $G(t)$, we track its co-occurrence with neighbors across communities from segments 1 to t, forming a temporal co-occurrence matrix $M_i^t \in \mathbb{R}^{N \times t}$. Each element $m_{ij}^t = 1$ if neighbor j belongs to the same community, and 0 if it belongs to

different community at time t. A shared multi-layer perceptron (MLP) encodes each historical segment $M_i^k \in \mathbb{R}^N$ independently, where $k = 1, \ldots, t$, followed by an aggregation operation to form a historical community-aware neighbor embedding h_i^t. The resulting matrix $H^t \in \mathbb{R}^{N \times D}$ is then concatenated with the zero-lagged node feature X_{fc}^t to generate the enhanced embedding $X_f^t \in \mathbb{R}^{N \times (N+D)}$.

2) Temporal-varying Representation Learning To capture long-range dependencies across networks, X_f^t are input to a Transformer Encoder[27] with l layers of multi-head self-attention (MHA) and feed-forward network (FFN) blocks:

$$\mathrm{MHA}(Q, K, V) = \mathrm{Concat}\big(\mathrm{head}_1, \ldots, \mathrm{head}_h\big) W_h, \tag{2}$$

$$\mathrm{FFN}(X) = \mathrm{GELU}\big(XW_1 + b_1\big) W_2 + b_2. \tag{3}$$

where $\mathrm{head}_i = \mathrm{Softmax}\big(QK^\top / \sqrt{d_h}\big)\, V$. The query, key, and value matrices Q, K, and V are obtained through learnable linear projections of the input features. W_h, W_1, W_2, b_1 and b_2 are learnable parameters. h is the number of attention heads, and d_h is the dimension of each head.

Inter-level Graph Learning To explore the brain's community structure and understand the dynamic patterns, we construct a community-level graph set $\mathcal{G} = \{\mathcal{G}_1, \mathcal{G}_2, \ldots, \mathcal{G}_C\}$, where C is the number of communities. For each community $c = 1, \ldots C$, its temporal graph $\mathcal{G}_c = \{V_c, A_c, X_c\}$ has $V_c = \{v_c^1, v_c^2, \ldots, v_c^T\}$, with each v_c^t representing community c at segment t. The feature matrix X_c is obtained by averaging the features of the nodes assigned to community c at each segment, and the adjacency matrix $A_c \in \mathbb{R}^{T \times T}$ is set to an all-ones matrix to indicate full temporal connectivity. After community aggregation, we stack two graph attention network (GAT) [28] layers on each community graph $\mathcal{G}_c$ to update temporal community-level features $X_c = \sigma\Big(\frac{1}{K} \sum_{k=1}^{K} W^k \tilde{x}_i^k\Big)$, where W^k is the learnable weight matrix, σ is a non-linear activation, and $\tilde{x}_i^k$ is the weighted aggregation of node i using attention coefficients α_{ij}.

$$\alpha_{ij} = \frac{\exp\Big(\psi\big(a^\top (W X_{c_i} \parallel W X_{c_j})\big)\Big)}{\sum_{k \in \mathcal{N}_i} \exp\Big(\psi\big(a^\top (W X_{c_i} \parallel W X_{c_k})\big)\Big)} \tag{4}$$

where a is a learnable weight vector, ψ is LeakyReLU function, $\parallel$ denotes concatenation, and $\mathcal{N}_i$ is the set of neighbors of node i. $X_c \in \mathbb{R}^{C \times T \times D'}$ are reshaped along time dimension T, and then fed to an MLP followed by sum pooling operation to obtain the graph-level representation $X_{intra} \in \mathbb{R}^{D'}$.

3 Experiments and Analysis

3.1 Datasets and Experiments Settings

The proposed method is evaluated on four datasets for three distinct brain disorder diagnosis tasks: (1) MCI diagnosis on ADNI dataset [11] from 134 cognitively

Table 1:
Classification results in terms of "mean (standard deviation)". The highest results are marked in **bold** and the second highest accuracies are underlined.

Metric	GAT	MVS-GCN	BrainGNN	ST2GCN	DAST-GCN	BISTFormer	BMR	STA-GIN	Ours
ADNI (CN vs. EMCI)									
ACC	0.585(0.018)	0.652(0.042)	0.715(0.058)	0.620(0.045)	0.665(0.052)	0.691(0.025)	0.712(0.050)	0.728(0.073)	**0.927(0.008)**
SEN	0.740(0.224)	0.896(0.063)	0.873(0.093)	0.630(0.217)	0.780(0.046)	0.711(0.046)	0.868(0.136)	0.758(0.119)	**0.940(0.032)**
SPE	0.374(0.294)	0.320(0.074)	0.500(0.112)	0.565(0.361)	0.502(0.130)	0.668(0.050)	0.496(0.240)	0.687(0.063)	**0.910(0.051)**
AUC	0.658(0.080)	0.608(0.046)	0.805(0.044)	0.637(0.091)	0.728(0.039)	0.700(0.032)	0.691(0.064)	0.801(0.095)	**0.925(0.012)**
F1	0.557(0.039)	0.591(0.050)	0.778(0.051)	0.597(0.095)	0.641(0.065)	0.808(0.020)	0.775(0.038)	0.758(0.074)	**0.937(0.007)**
ADNI (CN vs. LMCI)									
ACC	0.560(0.054)	0.634(0.029)	0.778(0.050)	0.617(0.046)	0.704(0.063)	0.669(0.028)	0.725(0.038)	0.691(0.057)	**0.852(0.040)**
SEN	0.585(0.285)	0.440(0.060)	0.761(0.109)	0.388(0.318)	0.526(0.125)	0.447(0.066)	0.556(0.154)	0.596(0.100)	**0.789(0.117)**
SPE	0.534(0.309)	0.791(0.062)	0.791(0.037)	0.750(0.278)	0.850(0.056)	0.850(0.052)	0.858(0.056)	0.768(0.057)	**0.903(0.060)**
AUC	0.507(0.132)	0.615(0.027)	0.828(0.062)	0.566(0.088)	0.609(0.096)	0.503(0.056)	0.703(0.037)	0.720(0.048)	**0.846(0.045)**
F1	0.560(0.037)	0.610(0.029)	0.750(0.069)	0.391(0.252)	0.688(0.062)	0.784(0.010)	0.633(0.111)	0.631(0.075)	**0.824(0.056)**
ABIDE (TC vs. ASD)									
ACC	0.541(0.028)	0.544(0.024)	0.558(0.021)	0.566(0.029)	0.619(0.032)	0.592(0.049)	0.619(0.024)	0.550(0.029)	**0.626(0.013)**
SEN	0.449(0.180)	0.321(0.126)	0.379(0.205)	0.555(0.244)	0.205(0.257)	0.236(0.201)	**0.565(0.121)**	0.500(0.090)	0.524(0.135)
SPE	0.620(0.196)	0.735(0.108)	0.695(0.226)	0.551(0.262)	0.865(0.167)	**0.898(0.089)**	0.659(0.098)	0.592(0.108)	0.713(0.123)
AUC	0.455(0.094)	0.528(0.026)	0.596(0.037)	0.512(0.125)	0.216(0.244)	0.567(0.061)	0.572(0.075)	0.503(0.043)	**0.618(0.015)**
F1	0.534(0.019)	0.505(0.045)	0.403(0.168)	0.528(0.037)	0.535(0.055)	0.237(0.240)	**0.625(0.025)**	0.561(0.039)	0.555(0.066)
ADHD (TC vs. ADHD)									
ACC	0.510(0.046)	0.617(0.029)	0.609(0.067)	0.569(0.088)	0.619(0.032)	0.659(0.006)	0.662(0.046)	0.586(0.034)	**0.677(0.023)**
SEN	**0.578(0.120)**	0.173(0.101)	0.410(0.153)	0.472(0.274)	0.205(0.257)	0.517(0.011)	0.263(0.184)	0.327(0.114)	0.403(0.100)
SPE	0.470(0.132)	0.905(0.040)	0.721(0.129)	0.612(0.285)	0.865(0.167)	0.744(0.005)	**0.905(0.070)**	0.742(0.093)	0.840(0.080)
AUC	0.465(0.040)	0.539(0.041)	0.606(0.058)	0.406(0.171)	0.216(0.244)	0.530(0.010)	0.603(0.042)	0.566(0.044)	**0.622(0.023)**
F1	0.524(0.029)	0.496(0.064)	0.474(0.057)	0.495(0.074)	0.535(0.055)	**0.631(0.007)**	0.339(0.169)	0.361(0.091)	0.475(0.068)
STAR (CU vs. MCI)									
ACC	0.648(0.046)	0.677(0.031)	0.600(0.094)	0.590(0.109)	0.669(0.046)	0.633(0.008)	0.712(0.042)	0.663(0.026)	**0.713(0.044)**
SEN	0.439(0.270)	0.225(0.076)	0.561(0.066)	0.479(0.303)	0.106(0.110)	0.402(0.008)	0.287(0.022)	0.351(0.200)	0.259(0.180)
SPE	0.748(0.182)	0.896(0.065)	0.320(0.262)	0.652(0.279)	**0.944(0.051)**	0.745(0.011)	0.917(0.030)	0.813(0.114)	0.930(0.077)
AUC	0.396(0.174)	0.560(0.029)	0.731(0.242)	0.386(0.156)	0.153(0.147)	0.407(0.008)	0.630(0.064)	0.378(0.114)	0.595(0.070)
F1	0.593(0.055)	0.547(0.036)	0.561(0.066)	0.530(0.101)	0.525(0.041)	0.573(0.007)	**0.395(0.041)**	0.685(0.044)	0.332(0.206)

normal (CN), 182 early MCI (EMCI), and 109 late MCI (LMCI) subjects, and a local dataset STAR from 230 cognitively unimpaired (CU) and 111 mild cognitive impairment (MCI) subjects; (2) autism spectrum disorder (ASD) diagnosis on ABIDE dataset [6] from 475 typical controls (TC) and 408 ASD subjects; and (3) attention deficit hyperactivity disorder (ADHD) diagnosis on ADHD-200 dataset [2] from 364 TC and 218 ADHD subjects. The Schaefer-500 atlas [25] is used to parcellate the brain into 500 ROIs. For ADNI, ABIDE, and STAR, the data preprocessing was conducted using DPARSF [31], while MRI data in ADHD-200 was preprocessed using the Athena pipeline[5].

For the training of CaDGNN, we use the Adam optimizer with a batch size of 20 and 50 epochs and learning rates 0.0001, 0.0001, $5e-5$ and 0.0001 on ADNI, STAR, ADHD-200 and ABIDE, respectively. Edges in graph set G are formed using k-nearest neighbor (knn) algorithm for the lag-aware matrices X^t_{lag} in Section 2.1. For the parameters, γ and ω in Eq. 1 are set to 1 and 0.1, embedding dimensions D and D' are set to 64 and 32, respectively. All the

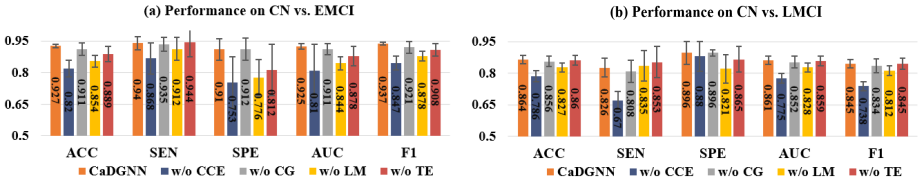

Fig. 2: The performance of CaDGNN and its variants on ADNI.

models are trained from scratch in an end-to-end manner with five-fold cross-validation using PyTorch on a single GPU (NVIDIA GeForce RTX 3090). Five metrics are used for a quantitative measurement: accuracy (ACC), sensitivity (SEN), specificity (SPE), F1 score, and area under ROC curve (AUC).

3.2 Experimental Results Comparison and Analysis

Comparison with the state-of-the-arts. The results on five binary classification tasks across different datasets are reported in Table 1. Compared with the best performing baselines, CaDGNN performs better by 27%, 9.5%, and 0.15% in accuracy on EMCI, LMCI and MCI diagnosis tasks, and by 4.3% on ABIDE and 2.7% on ADHD-200 in AUC. Besides, CaDGNN consistently outperforms static brain network analysis models (i.e., GAT [28], BrainGNN [15], MVS-GCN [30]) across all tasks in terms of accuracy. This is likely attributable to the fact that static methods rely solely on time-averaged FC, whereas CaDGNN explicitly integrates time delay information into dynamic FC modeling, thereby enhancing its capacity to capture both the heterogeneity and temporal evolution of brain activity. Additionally, Transformer-based methods (e.g., BISTFormer [13], BMR [29], and STA-GIN [12]) generally outperform GNN-only methods (e.g., ST2GCN [14], DAST-GCN [7]) in performance. This demonstrates the superior capacity of Transformer architectures to model complex spatiotemporal dependencies in brain networks. Notably, CaDGNN achieves significant improvements over comparative methods on ADNI, demonstrating that explicit integration of historical dynamic interactions enables more comprehensive characterization of both the topological organization and time-varying dynamics of BFC networks. Moreover, methods incorporating brain modularity priors (i.e., BMR and CaDGNN) consistently outperform those lacking explicit modular structure modeling. This suggests that embedding modularity priors into the modeling enhances the discriminability of dBFC graph representations for brain disorder diagnosis.

Ablation study. We conduct four variants of CaDGNN to perform the ablation study: (1) CaDGNN without the community-aware co-occurrence encoder (w/o CCE); (2) CaDGNN with the lag-aware dBFC construction process replaced by the zero-lagged construction method (w/o LM); (3) CaDGNN without the community graph construction during inter-level graph learning (w/o CG); and (4) CaDGNN without the Transformer Encoder (w/o TE).

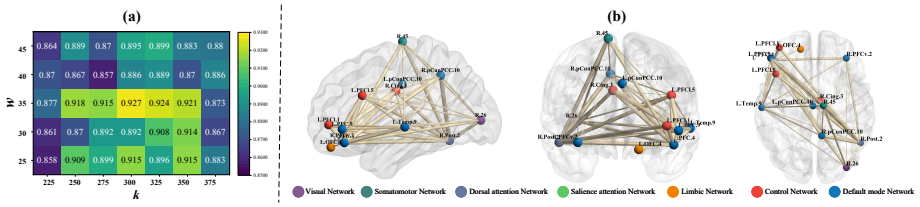

Fig. 3: (a) Performance of CaDGNN with different values of k and w. (b) Top-15 discriminative brain ROIs identified by CaDGNN on EMCI diagnosis task.

From the experimental results on ADNI presented in Fig. 2, we can see that removing either the CCE module or the lag-aware modeling component induces the most significant performance degradation. Specifically, CaDGNN w/o CCE and CaDGNN w/o LM exhibit relative accuracy drops of 4.1% and 7.5% on EMCI and LMCI diagnosis tasks, respectively. Notably, CaDGNN consistently outperforms all its variants, indicating that the components in CaDGNN exhibit complementary contributions to performance improvement and the collaborative learning at both ROI- and community-levels is critical for modeling dBFC networks. Furthermore, we investigate the sensitivity of CaDGNN to two key hyperparameters k and w, which jointly control the trade-off between spatial connectivity and temporal representations in dBFC graphs. As shown in Fig. 3 (a), darker colors indicate lower ACC values. CaDGNN achieves peak performance on EMCI diagnosis task when k is fixed at 300 and w is set to 35.

3.3 Visualization Analysis

To investigate the brain regions and their associated FCs identified by our method, we visualize discriminative regions based on learned network weights. As illustrated in Fig. 3(b), the most discriminative ROIs are primarily located within the Default Mode Network (DMN) and Control Network (Cont). This finding is consistent with previous studies indicating that brain regions within these large-scale networks are closely related to flexible node switching under different cognitive demands [32]. Moreover, abnormal functional connections anchored at these ROIs may reflect underlying pathological mechanisms contributing to EMCI diagnosis. For instance, the consistent finding of altered circuits between posterior cingulate (L.pCunPCC.10) and prefrontal cortex (L.PFC.4) reflects abnormal functional integration in EMCI subjects [8].

4 Conclusion

This paper introduces a novel framework named CaDGNN for brain disorder diagnosis. Leveraging time delay information extracted from rs-fMRI data, CaDGNN constructs dynamic brain graphs and jointly learns spatiotemporal

graph representations from both the ROI-level and community-level to support discriminative prediction. Notably, CaDGNN explicitly models the historical switching behavior of network nodes while embedding modularity priors into intra-level graph representation. Extensive experiments demonstrate that CaDGNN achieves superior performance across multiple diagnosis tasks and robustly identifies both the dynamic behaviors and topological properties of lag-based brain networks.

Acknowledgments. The work is supported by grants from Shenzhen Science and Technology Program (No. KCXFZ20211020163408012) and National Natural Science Foundation of China (No. 62006132).

Disclosure of Interests. The authors have no conflicts to disclose.

References

1. Avena-Koenigsberger, A., Misic, B., Sporns, O.: Communication dynamics in complex brain networks. Nature reviews neuroscience **19**(1), 17–33 (2018)
2. Bellec, P., Chu, C., Chouinard-Decorte, F., Benhajali, Y., Margulies, D.S., Craddock, R.C.: The neuro bureau adhd-200 preprocessed repository. Neuroimage **144**, 275–286 (2017)
3. Bolton, T.A., Morgenroth, E., Preti, M.G., Van De Ville, D.: Tapping into multifaceted human behavior and psychopathology using fmri brain dynamics. Trends in Neurosciences **43**(9), 667–680 (2020)
4. Chen, T., Li, H., Zheng, H., Fan, Y.: dfcexpert: Learning dynamic functional connectivity patterns with modularity and state experts. IEEE transactions on medical imaging (2025)
5. consortium, A..: The adhd-200 consortium: a model to advance the translational potential of neuroimaging in clinical neuroscience. Frontiers in systems neuroscience **6**, 62 (2012)
6. Craddock, C., Benhajali, Y., Chu, C., Chouinard, F., Evans, A., Jakab, A., Khundrakpam, B.S., Lewis, J.D., Li, Q., Milham, M., et al.: The neuro bureau preprocessing initiative: open sharing of preprocessed neuroimaging data and derivatives. Frontiers in Neuroinformatics **7**(27), 5 (2013)
7. El-Gazzar, A., Thomas, R.M., van Wingen, G.: Dynamic adaptive spatio-temporal graph convolution for fmri modelling. In: International Workshop on Machine Learning in Clinical Neuroimaging. pp. 125–134. Springer (2021)
8. Gili, T., Cercignani, M., Serra, L., Perri, R., Giove, F., Maraviglia, B., Caltagirone, C., Bozzali, M.: Regional brain atrophy and functional disconnection across alzheimer's disease evolution. Journal of Neurology, Neurosurgery & Psychiatry **82**(1), 58–66 (2011)
9. de Haan, W., van der Flier, W.M., Koene, T., Smits, L.L., Scheltens, P., Stam, C.J.: Disrupted modular brain dynamics reflect cognitive dysfunction in alzheimer's disease. Neuroimage **59**(4), 3085–3093 (2012)
10. Hu, J., Du, J., Xu, Q., Yang, F., Zeng, F., Weng, Y., Dai, X.j., Qi, R., Liu, X., Lu, G., et al.: Dynamic network analysis reveals altered temporal variability in brain regions after stroke: A longitudinal resting-state fmri study. Neural plasticity **2018**(1), 9394156 (2018)

11. Jack Jr, C.R., Bernstein, M.A., Fox, N.C., Thompson, P., Alexander, G., Harvey, D., Borowski, B., Britson, P.J., L. Whitwell, J., Ward, C., et al.: The alzheimer's disease neuroimaging initiative (adni): Mri methods. Journal of Magnetic Resonance Imaging: An Official Journal of the International Society for Magnetic Resonance in Medicine **27**(4), 685–691 (2008)
12. Kim, B.H., Ye, J.C., Kim, J.J.: Learning dynamic graph representation of brain connectome with spatio-temporal attention. Advances in Neural Information Processing Systems **34**, 4314–4327 (2021)
13. Li, L., Zhang, L., Cao, P., Yang, J., Wang, F., Zaiane, O.R.: Exploring spatio-temporal interpretable dynamic brain function with transformer for brain disorder diagnosis. In: International Conference on Medical Image Computing and Computer-Assisted Intervention. pp. 195–205. Springer (2024)
14. Li, S., Zhu, Q., Tian, C., Shao, W., Zhang, D.: Interpretable dynamic brain network analysis with functional and structural priors. IEEE Transactions on Medical Imaging (2025)
15. Li, X., Zhou, Y., Dvornek, N., Zhang, M., Gao, S., Zhuang, J., Scheinost, D., Staib, L.H., Ventola, P., Duncan, J.S.: Braingnn: Interpretable brain graph neural network for fmri analysis. Medical image analysis **74**, 102233 (2021)
16. Li, Y., Yu, D., Liu, Z., Zhang, M., Gong, X., Zhao, L.: Graph neural network for spatiotemporal data: methods and applications. arXiv preprint arXiv:2306.00012 (2023)
17. Ma, Y., Wang, Q., Cao, L., Li, L., Zhang, C., Qiao, L., Liu, M.: Multi-scale dynamic graph learning for brain disorder detection with functional mri. IEEE Transactions on Neural Systems and Rehabilitation Engineering **31**, 3501–3512 (2023)
18. Mijalkov, M., Veréb, D., Canal-Garcia, A., Hinault, T., Volpe, G., Pereira, J.B., Initiative, A.D.N.: Nonlinear changes in delayed functional network topology in alzheimers disease: relationship with amyloid and tau pathology. Alzheimer's Research & Therapy **15**(1), 112 (2023)
19. Mitra, A., Snyder, A.Z., Blazey, T., Raichle, M.E.: Lag threads organize the brains intrinsic activity. Proceedings of the National Academy of Sciences **112**(17), E2235–E2244 (2015)
20. Mitra, A., Snyder, A.Z., Hacker, C.D., Raichle, M.E.: Lag structure in resting-state fmri. Journal of neurophysiology **111**(11), 2374–2391 (2014)
21. Mucha, P.J., Richardson, T., Macon, K., Porter, M.A., Onnela, J.P.: Community structure in time-dependent, multiscale, and multiplex networks. science **328**(5980), 876–878 (2010)
22. Pei, S., Ma, J., Lv, Z., Zhang, C., Guan, J.: Community-aware graph transformer for brain disorder identification. In: Proceedings of the Thirty-Fourth International Joint Conference on Artificial Intelligence. pp. 4191–4199 (2025)
23. Raut, R.V., Mitra, A., Snyder, A.Z., Raichle, M.E.: On time delay estimation and sampling error in resting-state fmri. Neuroimage **194**, 211–227 (2019)
24. Rubinov, M., Sporns, O.: Weight-conserving characterization of complex functional brain networks. Neuroimage **56**(4), 2068–2079 (2011)
25. Schaefer, A., Kong, R., Gordon, E.M., Laumann, T.O., Zuo, X.N., Holmes, A.J., Eickhoff, S.B., Yeo, B.T.: Local-global parcellation of the human cerebral cortex from intrinsic functional connectivity mri. Cerebral cortex **28**(9), 3095–3114 (2018)
26. Varga, L., Moca, V.V., Molnar, B., Perez-Cervera, L., Selim, M.K., Díaz-Parra, A., Moratal, D., Pentek, B., Sommer, W.H., Murean, R.C., et al.: Brain dynamics supported by a hierarchy of complex correlation patterns defining a robust functional architecture. Cell Systems **15**(8), 770–786 (2024)

27. Vaswani, A., Shazeer, N., Parmar, N., Uszkoreit, J., Jones, L., Gomez, A.N., Kaiser, Ł., Polosukhin, I.: Attention is all you need. Advances in neural information processing systems **30** (2017)
28. Velickovic, P., Cucurull, G., Casanova, A., Romero, A., Lio, P., Bengio, Y., et al.: Graph attention networks. stat **1050**(20), 10–48550 (2017)
29. Wang, Q., Wang, W., Fang, Y., Yap, P.T., Zhu, H., Li, H.J., Qiao, L., Liu, M.: Leveraging brain modularity prior for interpretable representation learning of fmri. IEEE Transactions on Biomedical Engineering **71**(8), 2391–2401 (2024)
30. Wen, G., Cao, P., Bao, H., Yang, W., Zheng, T., Zaiane, O.: Mvs-gcn: A prior brain structure learning-guided multi-view graph convolution network for autism spectrum disorder diagnosis. Computers in biology and medicine **142**, 105239 (2022)
31. Yan, C.G., Wang, X.D., Zuo, X.N., Zang, Y.F.: Dpabi: data processing & analysis for (resting-state) brain imaging. Neuroinformatics **14**(3), 339–351 (2016)
32. Yi, C., Fan, Y., Wu, Y.: Cross-module switching diversity of brain network nodes in resting and cognitive states. Cognitive Neurodynamics **17**(6), 1485–1499 (2023)
33. Zhou, L., Jiang, Z., Chang, Z., Wang, R., Wu, Y.: Spatiotemporal transition of resting-state brain networks associates with human cognitive abilities. Cognitive Neurodynamics **19**(1), 1–14 (2025)